



Recent changes in extreme wave events in the south-western South Atlantic

Carolina B. Gramcianinov¹, Joanna Staneva¹, Celia R. G. Souza^{2,3}, Priscila Linhares³,
Ricardo de Camargo⁴, and Pedro L. da Silva Dias⁴

¹Institute for Coastal Systems Analysis and Modeling, Helmholtz-Zentrum Hereon, Max-Planck-Straße 1,
21502 Geesthacht, Germany

²Institute of Environmental Research, Secretariat of Environment, Infrastructure and Logistics of São Paulo
State (SEMIL/SP), Rua Joaquim Távora 822, 04015-011, São Paulo – SP, Brazil

³Department of Physical Geography, Faculty of Philosophy, Literature and Human Sciences, University of São
Paulo (FFLCH/USP), Av. Prof. Lineu Prestes, 338, 05508-000, São Paulo – SP, Brazil

⁴Department of Atmospheric Sciences, Institute of Astronomy, Geophysics and Atmospheric Science,
University of São Paulo, Rua do Matão, 1226, 05508-090, São Paulo – SP, Brazil

Correspondence: Carolina B. Gramcianinov (carolina.gramcianinov@hereon.de)

Received: 31 July 2022 – Discussion started: 23 September 2022

Revised: 8 March 2023 – Accepted: 31 March 2023 – Published: 27 September 2023

Abstract. Over the past decades, the South Atlantic Ocean has experienced several changes, including a reported increase in coastal erosion and floods. This study aims to investigate the recent changes in the extreme wave events over the south-western South Atlantic (SWSA) – which hosts the most economically important harbours in South America, high oil and gas production demands, and rich biodiversity. This investigation considers not only the occurrence of extreme wave events but also extreme wave indicators that characterise the potential wave impact on offshore and coastal areas. Extreme wave events are obtained using the averaged monthly 95th percentile of significant wave height (H_s) from 1993 to 2021, combining the CMEMS global wave reanalysis and near-real-time products. Annual and seasonal statistics are derived to analyse mean and extreme wave climate and trends in the study region, focusing on H_s , peak period, and wave power. The analysis gives an overview of the wave climate in the study domain, including a discussion about seasonal differences. For a more direct application to future risk assessment and management, we perform an analysis considering the regional monitoring and warning system division established by the Brazilian Navy. We used a coastal hazard database that covers a portion of the coast to investigate how the trends given by the CMEMS wave products may impact the coastal zone. Our findings showed significant changes in the SWSA mainly associated with an increase in mean values of H_s , wave period, and consequently the wave power. Narrowing down to the coastal impact, we found an increase in the number of coastal hazards in the State of São Paulo associated with waves, which agrees with the increase in the number of extreme wave events in the adjacent ocean sector. However, the increased number of coastal events is also driven by local factors.

1 Introduction

In recent years, several extreme events have been reported in the South Atlantic Ocean (e.g. Marcello et al., 2018; Dalagnol et al., 2022), thus directly reflecting hazards along the coast. One of the regions that are facing relevant changes is the south-western South Atlantic (SWSA), with an increase in extreme wave and storm surge occurrences (Souza et al., 2019; Gramcianinov et al., 2023). With high economic relevance, the SWSA region hosts strategic harbours in South America, where 7.55×10^8 t of goods were transported in 2021 (ANTAQ, 2022), and promising oil and gas exploration fields. In addition, the region also holds rich biodiversity, including coral reefs and 856 km² of mangroves that are crucial for coastal hazard protection, economic activities (e.g. fishery), and the cultural identity of the coastal communities (ICMBio, 2018; Pereira-Filho et al., 2021). The SWSA coastal cities have a dense population, with approximately 20 million people who are extremely vulnerable to coastal erosion and infrastructure damage (Zamboni and Nicolodi, 2008).

Assessing the extreme waves and wave trends in the SWSA with traditional approaches has proven to be challenging for several reasons. The difficulties remain mostly in the still-limited understanding of the local physical processes (e.g. wave–current interaction) and climate variabilities (e.g. the overlapping effect teleconnections). The limited accuracy of long-term integrations and the scarce data availability can make these analyses even more difficult. Some recent studies have revealed changes in the wave pattern in the South Atlantic, usually ascribed to the increase in the extreme waves in the Southern Ocean (SO). In general, previous global or hemisphere-based studies have reported increases in wave height extremes in the Southern Hemisphere (SH) over the past 41 years, and this tendency is expected to continue in the future (Caires and Sterl, 2005; Dobrynin et al., 2012; Lemos et al., 2019). However, when focusing on the SWSA, the mean and extreme wave climate trends present larger uncertainties.

In addition to understanding the significant wave height (H_s) trends, assessing changes in wave event characteristics, such as the mean wave direction and peak period, is of utmost importance. Silva et al. (2020) showed how the oscillation between the southern and eastern dominant wave energy flux directions has led to changes in the coastal morphodynamics at both regional and local scales. Some previous works reported wave power changes under the present climate (Odériz et al., 2021; 1979–2018) and mean wave direction and period changes in both present (Hemer et al., 2010; 1989–2005) and future climate (Lobeto et al., 2021; 2081–2100). These changes directly affect naval and coastal risk assessments, requiring special efforts to properly link the global-scale findings to regional and local wave extremes.

Against such a background, this section aims to report and investigate the recent extreme wave climate trends (1993–

Table 1. Copernicus Marine Service (CMEMS) and non-CMEMS products used in this study, including the Quality Information Document (QUID) and Product User Manual (PUM).

Product ref. no.	Product ID and type	Data access	Documentation
1	GLOBAL_MULTITYEAR_WAV_001_032 (WAVERYYS), numerical models	EU Copernicus Marine Service Product (2021)	QUID: Law-Chune et al. (2021b); PUM: Law-Chune (2022)
2	GLOBAL_ANALYSIS_FORECAST_WAV_001_027 (GLO-NRT), numerical models	EU Copernicus Marine Service Product (2022)	QUID: Aouf (2022); PUM: Dalphinnet et al. (2022)
3	Baixada Santista Coastal Hazards database (BDe-BS), dataset	Personal contact	Souza et al. (2019, 2022)

2021) in the SWSA while focusing on wave event characteristics such as event frequency, intensity, duration, and peak period. We examined the seasonal statistics and climatic trends using both traditional (i.e. percentile-based) and storm-based approaches to provide new insights into the regional wave climate changes. To obtain results with more direct application to future risk assessment and management, we performed an analysis considering the regional monitoring and warning system, as well as the impact of the recent wave climate changes on the coast.

2 Methods

2.1 Datasets

The main dataset used in this work was the Copernicus Marine Service (CMEMS) global reanalysis, named WAVERYS (product ref. no. 1; Table 1; Law-Chune et al., 2021a), available from 1993 to 2020. To include 2021 in the analysis, the WAVERYS was complemented with data from the CMEMS Global Ocean Waves Analysis Near Real Time product (GLO-NRT; product ref. no. 2; Table 1). The combination (in time) of these two products is hereafter referred to as CMEMS wave products. WAVERYS is available at a $1/5^\circ$ horizontal grid as 3-hourly outputs from 1993 to 2020, while the wave analysis has a $1/12^\circ$ horizontal grid as 3-hourly instantaneous output fields. The GLO-NRT product was interpolated to the 0.20° horizontal grid, so a more consistent analysis can be achieved despite using different sources. Both products are produced using the Météo-France Wave Model (MFWAM) with the dissipation terms developed by Ardhuin et al. (2010). WAVERYS is forced by hourly surface winds and daily sea-ice fraction fields derived from the fifth-generation reanalysis from the European Centre for Medium-Range Weather Forecasts (ECMWF) (ERA5; Hersbach et al., 2020) and ocean currents obtained from the ocean reanalysis Global Ocean Reanalysis and Simulation (GLORYS). The GLO-NRT is forced only by a 6-hourly wind analysis from the IFS-ECMWF atmospheric system.

An evaluation of WAVERYS for the western South Atlantic wave climate was made by Crespo et al. (2022). The authors compared H_s from the WAVERYS, ERA5, and the National Centers for Environmental Prediction (NCEP) wave reanalysis (Chawla et al., 2013) against wave buoy measurements at three locations along the Brazilian coast and found that WAVERYS presented the highest correlation and the lowest root mean square deviation (RMSD). The ERA5 performance in representing the winds is also relevant as the quality of the forcing field is crucial in a wave simulation. Previous works have shown that ERA5 can represent the wind climate, extreme percentiles, and storm variability (e.g. Belmonte Rivas and Stoffelen, 2019; Gramscianinov et al., 2020a; Crespo et al., 2022).

2.2 Percentile computation

In this work, the percentiles were computed using the empirical distribution of the H_s peaks ($H_{s\text{peaks}}$) within a given period, thus allowing us to obtain a more detailed view of individual wave events' occurrence. The selected $H_{s\text{peaks}}$ must be separated by a minimum of 48 h to guarantee the independence of the peaks. This time window has been widely applied in past studies to ensure the collection of one peak per storm (e.g. Caires and Sterl, 2005; Meucci et al., 2020). Besides that, 48 h is a suitable but not so restrictive time threshold for extreme-wave analysis in the region, particularly considering the differences among the seasons. The 95th percentile was computed based on the monthly $H_{s\text{peaks}}$ distribution at each grid point. Using these monthly 95th percentiles, we calculated the annual and seasonal means to analyse trends and proceed with the wave event analysis (Sect. 2.4). The seasonal mean of the monthly 95th percentiles was computed for the summer and winter, using the average December–January–February (DJF) and June–July–August (JJA), respectively, thus having one value per year. The annual percentiles were computed by the average of all monthly percentiles within the year. As a final result, we have a mean annual and seasonal percentile time series at each grid point.

2.3 Trend estimation and testing

Trends were estimated based on Sen's slope estimator (Sen, 1968), which evaluates the magnitude of a time series trend. The significance of Sen's slope was calculated by the Mann–Kendall test (Mann, 1945; Kendall, 1975), considering a p value lower than 0.05. Both methods are non-parametric (distribution-free) procedures and consider the monotonic increase upward or downward of the time series, thus being more robust to climate-based analysis (e.g. Wang et al., 2020).

2.4 Extreme-wave-event analysis

The wave event statistics were derived following the methods developed by Weisse and Günther (2007), in which consecutive points over a specific threshold within a given time series are considered to define extreme wave events. This event-counting process was performed for each grid cell considering its unique severe event threshold (SET), defined herein as the average of the monthly 95th percentile of $H_{s\text{peaks}}$ considering the whole period (1993–2021). Notably, there is no widely accepted method for selecting threshold values, and values between the 90th and 99th percentile H_s are often used (De Leo et al., 2020; Gramscianinov et al., 2020b). Moreover, the use of the averaged monthly percentile results in a smoothed field, especially due to the $H_{s\text{peaks}}$ variability among the year. In this way, for some locations, the exceedance of events above SET was larger than 5 %.

Following Weisse and Günther (2007), the intensity is equal to the difference between the maximum H_s of the event and the SET at that point. The wave event statistics, such as the number of events, intensity, mean wave direction, and peak period, are presented herein as annual and seasonal means to build the spatial distribution and trends and obtain the spatially averaged time series. The intensity and wave parameters were calculated by averaging all individual events (above SET) within the year or season. The same analysis was applied successfully in the Black Sea by Staneva et al. (2022), allowing a better understanding of the extreme wave events' spatial distribution and trends. More details about these methods can be found in Weisse and Günther (2007).

2.5 Wave power calculation

Following Staneva et al. (2022), we also calculated the wave power in the study domain. Wave power or wave energy flux was obtained following Eq. (1):

$$P = \left(\frac{\rho g^2}{64 \pi} \right) H_s^2 T_e, \quad (1)$$

where P is the wave energy flux per unit of wave-crest length (kW m^{-1}), ρ is water density, g is the acceleration due to gravity, H_s is the significant wave height, and T_e is the wave energy period. T_e is directly available in the WAV-ERYS products (named VTM10) and is defined as the mean wave period obtained by the $T_e \equiv T_{m-1,0} = m_{-1}/m_0$, based on the -1 th and 0 th moment of the wave spectrum.

2.6 Coastal risk assessment

Warnings and risk assessment in this region are supervised by the Centre of Hydrography of the Brazilian Navy (CHM, from *Centro de Hidrografia da Marinha*), which is recognised by the World Meteorological Organization (WMO) as the issue service for the MetArea V (Atlantic waters west of 7°N – 35.8°S , 20°W). According to the CHM monitoring system, the coastal region of SWSA can be divided into four subareas (Fig. 1). These subareas were used to analyse the wave climate trends in the domain, considering the regional specificity and facilitating future discussions about risk management. This analysis may facilitate the applicability of the results found here to improve future monitoring and warning system development.

We used a historical database of coastal hazards in the State of São Paulo, within subarea C, to further investigate coastal impacts. The Baixada Santista Coastal Hazards database (BDe-BS; product ref. no. 3; Table 1) covers the period from 1928 to 2021 and is obtained using the hemerographic method (mostly newspapers) and material from social media (mostly videos), showing coastal impacts caused by strong waves and anomalously high tides (either meteorological or astronomical tides) (Souza et al., 2019; Linhares

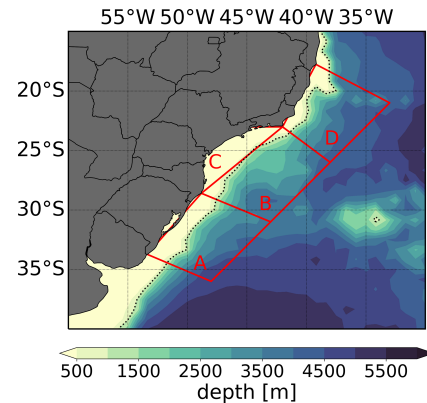


Figure 1. The south-western South Atlantic Ocean with subareas A to D defined by the Brazilian Navy for warning and monitoring operations within MetArea V. Shaded values are the bathymetry from ETOPO1.

et al., 2021; Souza et al., 2022). The definition of coastal hazards is mainly based on processes such as coastal erosion and/or coastal inundation, the latter also forced by continental flooding (heavy rainfall) in estuarine areas. Therefore, the coastal hazards registered in the BDe-BS represent events with high intensity since they were brought to the attention of the public due to their significant impact on the beaches, destruction of urban structures, and public and private properties, as well as disruption of the city's day-to-day and port activities. More details regarding the database can be found in Souza et al. (2019).

Currently, the BDe-BS initiative is maintained by the São Paulo state government through the “Preventive Plan for Coastal Erosion, Coastal Inundation, and Flooding” (adapted from the Portuguese: *Plano Preventivo de Defesa Civil para Erosão Costeira, Inundações Costeiras e Enchentes/Alagamentos causadas por Eventos Meteorológicos-Oceanográficos Extremos como Ressacas do Mar e Marés Altas*). Despite representing a small portion of the coastal area of the SWSA, the number of intense/extreme events reaching the São Paulo state coast can be considered representative of most of the coastal extension of the domain in this study, except for subarea D (see Fig. 1). The reason for this extrapolation is mainly the lack of long-term records in other locations. In addition, the database covers the central portion of the study region in a region with high economic importance.

3 Results

3.1 Extreme-wave-climate characterisation

The 95th percentile distribution, with its gradient towards the south (Fig. 2a, e, i) followed by the concentration of more intense extreme events to the southern portion of the domain (Fig. 2c, g, k), reflects the influence of the South Atlantic

storm track in the region. The storm track controls the extreme wave climate in the SWSA due to the strongest winds associated with the cyclones (e.g. Campos et al., 2018), and it is located between 55 and 30° S (Hoskins and Hodges, 2005; Gramscianinov et al., 2019).

Despite sharing a common extreme-wave-generation source, as is possible to see by the similar mean-wave-direction distribution (Fig. 2d, h, l), summer (DJF) and winter (JJA) present distinct wave patterns due to the southward shift in the storm track in the summertime (Hoskins and Hodges, 2005). Thus, the summer presents smaller values of H_s – and consequently 95th percentile $H_{s_{\text{peaks}}}$ ($H_{s_{p95}}$ hereafter) values (Fig. 2e) – in the study domain, which is reflected a lower number of events (Fig. 2f) and weaker events (Fig. 2g) than winter and the whole period. Climatologically, the austral autumn (MAM) presents behaviour closer to the summer pattern, while spring (SON) and winter patterns are similar. In this study, we further analyse the whole period and winter since summer does not present many cases.

During the winter, the main storm track is in its northernmost position (Hoskins and Hodges, 2005), resulting in more wave events than in other seasons (Fig. 2j). Typically, in winter, the region presents relatively long fetches along the coast (south-west-/north-east-oriented) associated with cyclones generated at approximately 35° S (Gramscianinov et al., 2021). These fetches can be widely intensified by rear anticyclones on the western side of the cyclone, thus causing this configuration to be widely related to the most severe cases observed in the domain (e.g. da Rocha et al., 2004; Machado et al., 2010; Dragani et al., 2013).

The high number of events in the northern boundary of the domain (Fig. 2b, j) can be associated with the South Atlantic Subtropical High (SASH), which is also a generating system in the study region (Pianca et al., 2010). The SASH mostly influences the wave climate by generating easterly waves towards central Brazil, northward from 23° S. However, the wave events in this location are associated with relatively small H_s , as is possible to see by the local $H_{s_{p95}}$ values (Fig. 2a, i) and wave event intensities (Fig. 2c, k). For instance, the $H_{s_{p95}}$ values in the northern portion of the domain do not reach 3.5 m in the winter (Fig. 2i).

The overall pattern and values presented in Fig. 2 agree with previous studies, even though methodological differences exist, thus making a straightforward comparison difficult. For instance, Gramscianinov et al. (2020b), using the 90th percentile computed through a spatially varying time window, found a mean of 1.3 and 5.5 extratropical cyclones per year associated with extreme wave events in the region in the summer and winter, respectively. These values are comparable with the number of events presented in the maps of Fig. 2b, g, and l. Regarding the intensity, the same authors found a mean H_s of 6.5 m associated with these cyclone events, which is also comparable to the intensity values (above the percentile) in some locations of the study domain (Fig. 2c, h, m). Moreover, Machado et al. (2010) accessed

extreme wave events in the coastal region between 30° S and 32° S and found a mean of 1.33 events per year above the 90th percentile between 1979 and 2008. We also reported this relatively small value at this exact location in Fig. 2b, g, and l. In this way, the method applied herein presents robust results according to what is reported in the region.

3.2 Extreme wave event trends

The monthly $H_{s_{p95}}$ trends present a sparse and weak signal in the study domain, except for the winter (Fig. 3f). The southern coast presents a significant increase in the $H_{s_{p95}}$ values, which are greater than 2 cm yr^{-1} in some locations during the wintertime. When looking at the mean H_s trend, it is possible to see a general increase in this wave parameter along the Brazilian continental shelf, covering the coastal and offshore regions. The magnitude of the mean H_s increase is small ($< 0.2 \text{ cm yr}^{-1}$) but significant in the whole period (Fig. 3b). The mean H_s increase in winter is relatively greater (between 0.4 and 0.8 cm yr^{-1} ; Fig. 3g). The differences between the mean and $H_{s_{p95}}$ trend signal are in agreement with the findings of Young and Ribal (2019), who showed that the H_s distribution changes in the last years were skewed to the left, with an increase in small waves – which can change the mean without changing the extreme percentiles. The trends in the number of extreme wave events also present sparse behaviour, but with significant increases along the Brazilian coast (Fig. 3c, h). The event increase occurs on most of the coast in the whole-period analysis, while it is confined to some portions of the southern and south-eastern coast during the winter (Fig. 3h). It is important to note that the rise in the number of events does not follow the $H_{s_{p95}}$ trend pattern.

Figure 3 also shows the spatial trends of the mean distribution of the wave peak period and wave power during the events (Fig. 3d, e, i, j). There is a general increase in the peak period in the study domain, confined to the central portion of the coast in the winter (Fig. 3i). The increase in wave period and H_s can lead to important changes in the wave power (Eq. 1). Note that for the wave power calculation, T_e was used, and the trends presented in Fig. 3d and i are based on the T_p . However, considering a JONSWAP wave spectrum, T_e is directly related to T_p ($T_e = 0.9 \times T_p$; Guillou, 2020). The wave power presents a small but significant increase along the coast in the whole period and wintertime (Fig. 3e, j), reaching maximum values ($> 0.2 \text{ kW m}^{-1} \text{ yr}^{-1}$) offshore of the southern Brazilian and Uruguayan coast (30–40° S) in the winter. Following the mean H_s behaviour, the increase in the wave power is larger in the winter than in the whole period – as expected, as wave power is proportional to H_s^2 (Eq. 1). Other extreme event indicators, such as intensity, mean wave direction, and lifetime, did not present a robust trend signal and, therefore, are not shown.

The extreme-event analysis based on each grid point in a high-resolution hindcast provides a more detailed view of pattern changes along the coast. On the other hand, such an

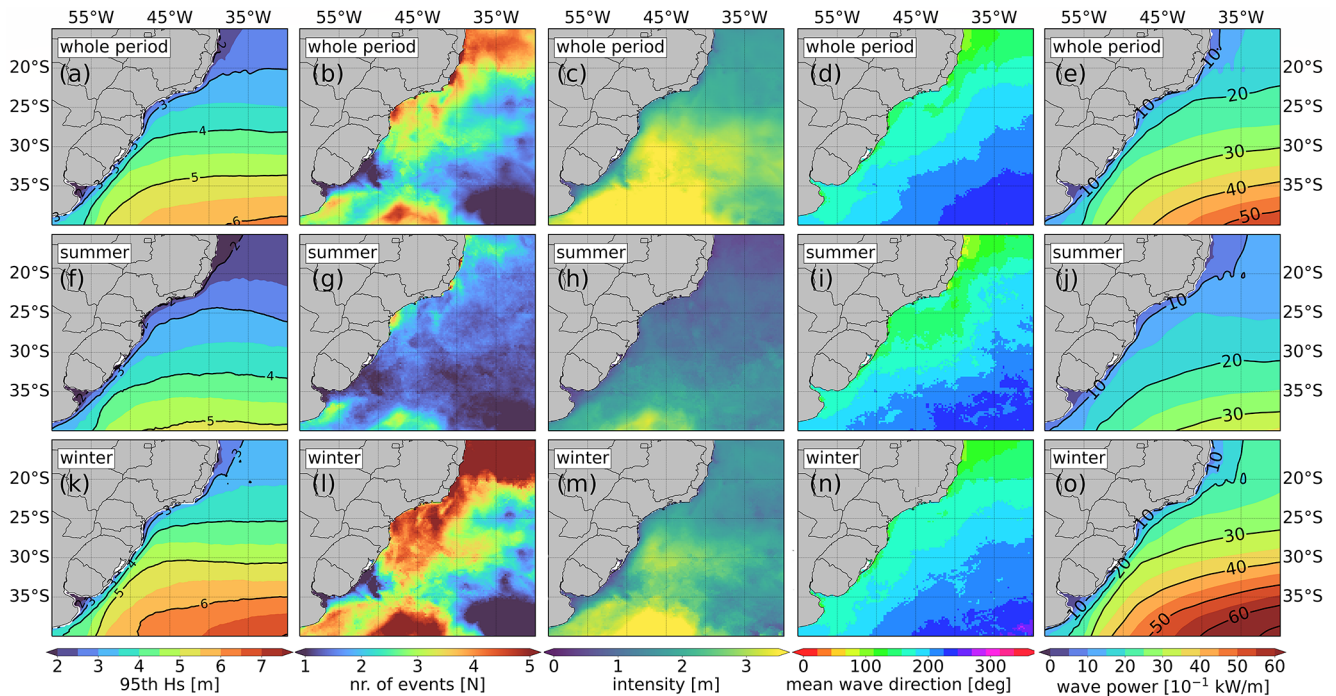


Figure 2. (a, f, k) Averaged monthly 95th percentile $H_{s_{\text{peaks}}}$ value (m), (b, g, l) extreme-wave-event number, (c, h, m) intensity ($H_{s-95\text{th}} H_{s_{\text{peaks}}}$) (m), (d, i, n) mean direction (degrees), and (e, j, o) mean wave power ($10^{-1} \text{ kW m}^{-1}$) in (a–e) the whole period (1993–2021), (f–j) summer (DJF), and (k–o) winter (JJA) based on the CMEMS wave products (product ref. nos. 1 and 2; Table 1).

analysis can produce sparse results that may not be easily applied to more practical and operational tasks. Therefore, the trends in some event parameters were analysed for each Brazilian Navy monitoring and warning subarea (Fig. 4). For this analysis, we focused on the parameters with significant trends in at least one region and season, although both whole-period and winter trends are presented in Fig. 4 for consistency. Both subareas C and D present a significant increase in the number of events in the whole period. The trends of 0.2 and 0.28 events per year represent an increase of $\sim 20\%$ in subareas C and D in 29 years (based on the increase in the annual mean of their series). Together with subarea B, these regions also present an increase in the mean wave power – despite no significant change in the peak period. In the winter, subareas A and C present significant trends in the number of events per year, representing a 27.2% and 20% increase, respectively. Subarea C presents a small but significant increase in peak period in the winter, as well as in the wave power. The wave power also increases in subarea D in the winter.

By the time series, it is possible to note a high interannual variability due to large-scale climate modes that affect the regional wave climate through storm track shifts (e.g. Sasaki et al., 2021). The SWSA is affected by many large-scale variability modes that interact, which are widely studied in the atmosphere but not well understood in the wave fields (Godoi et al., 2020; Godoi and Torres Júnior, 2020; Sasaki et al.,

2021), which make it difficult to correlate climate indexes with wave parameters directly. However, even considering these variabilities, most parameters present a positive trend, although not always significant. As explained in Sect. 2.3, we consider the Mann–Kendall test to assess the significance of the trends. The sensitivity of the Mann–Kendall test may be related to the large variance of the time series, which directly influences the trend detected by this method (Wang et al., 2020).

3.3 Coastal risk analysis

The Charlies subarea (C) is one of the most affected locations, experiencing an increased number of extreme wave events, peak periods, and wave power in the last years. However, linking the changes in the regional wave climate with coastal hazards is not a straightforward task as the wave systems are modified by bathymetry, and their impact depends on the coastal morphodynamics. Table 2 presents the number of events recorded by the BDe-BS and the computed trends for each type of hazard. The São Paulo coast was affected by 163 hazards between 1993 and 2021, of which 48% (78) were caused exclusively by storm waves and 30% (49) by the combination of waves and tides (as a result of either astronomical or meteorological tides). In the winter, 93% (51) of events are associated with waves, with combined events showing a similar proportion (35%) of total events com-

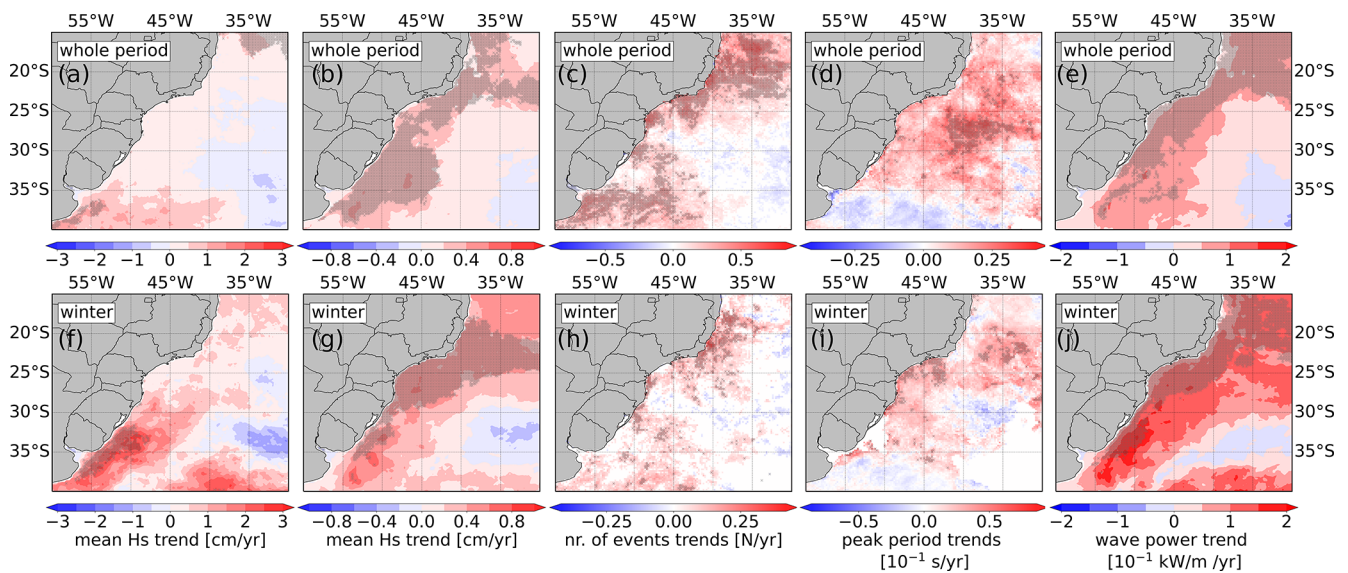


Figure 3. Trends in the (a, f) 95th percentile $H_{s\text{speaks}}$ (cm per year), (b, g) mean H_s (cm per year), (c, h) number of extreme wave events (number per year), (d, i) peak period of the events ($10^{-1} \text{ s yr}^{-1}$), and (e, j) mean wave power ($10^{-1} \text{ kW m}^{-2} \text{ yr}^{-1}$) in the (a–e) whole period and (f–j) winter (JJA) based on the CMEMS wave products (product ref. nos. 1 and 2; Table 1). Grey crosses represent points where the trend is significant (Mann–Kendall test, p value ≤ 0.05).

pared to the whole period (30%). Thus, the hazards forced exclusively by anomalous tides are rare in the winter, which may be related to the high wave event frequency in this season. The number of events on the coast increased both for the whole period and in winter (JJA). The increase in the number of coastal hazards was mainly led by wave events since events caused only by tidal influence did not present any significant trend. The results show an increase of 120% and 145% of total events and wave-forced events on the coast in 29 years, considering the whole-period mean. This high increase is in agreement with Souza et al. (2019), who found a pronounced increase in wave-forced hazards after the decades 2000–2009 and 2010–2019 (226% compared with the 1928–1999 period) when analysing a longer period of the same database (1928–2016).

Figure 5 shows the time series of the yearly events of coastal hazards from the BDe-BS against the spatial sum of the number of events in subarea C obtained by the wave event analysis (described in Sect. 2.4). Due to the small number of coastal hazards per year, we show the time series and trends for the whole period to obtain more robust statistics. Nevertheless, the winter trends presented the same signal and relation among the event types as the whole period trends (see Table 2). Note that the absolute numbers of events recorded on the coast and obtained in subarea C are not comparable. This analysis aims to evaluate the similarity in the variability and trends of the time series. The number of events presented for subarea C in Fig. 5 is the sum of events in all grid points within defined boundaries.

Most of the coastal hazards reported by the BDe-BS are associated with waves, combined or not with a tidal rise. This is revealed by the numbers not only in Table 2 but also in the time series (Fig. 5a). The trends of all events and events associated with waves are similar, especially considering the trend error. It is possible to compare the trends in the coastal hazards forced by waves (0.22 events per year; Table 2) with the trends of the number of extreme wave events in subarea C (Fig. 5b; 0.20 events per year in Fig. 4a). However, considering the mean number of coastal events forced by waves (4.4 events per year), the increase on the coast corresponds to 145% in 29 years.

Although there is no total agreement between the extreme events detected in subarea C and hazards reported on the coast in the year-by-year analysis, the trend behaviour is similar. The number of combined events (wave + tides) and the total event trend are superposed in Fig. 5b. These overlaid pictures show that differences in the wave-forced coastal hazards and extreme wave events in subarea C may result from the influence of sea-level-elevation events forced by storms or astronomical tides. For instance, 2002 and 2009 do not present a peak in the extreme wave events within subarea C, but they were marked by a high number of wave-forced coastal hazards related to a higher percentage of combined events. These wave events would not become a hazard if the local sea level elevation did not allow waves to reach further into the continental area. In addition, the disagreement between the coastal and offshore event time series can be addressed for bathymetry and morphology reasons.

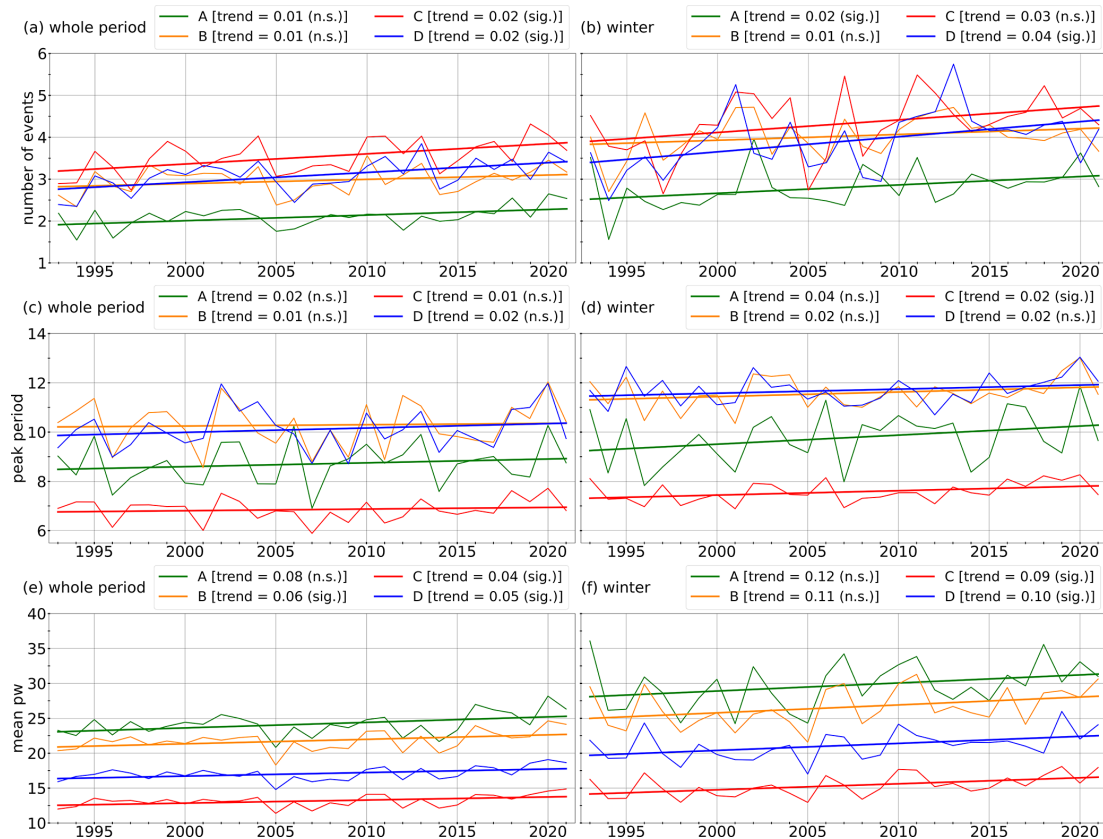


Figure 4. Annual time series and trends for the (a, b) number of extreme wave events (number per month), (c, d) mean peak period of the events (s), and (e, f) mean wave power ($10^{-1} \text{ kW m}^{-1}$) in the (a, c, e) whole period and (b, d, f) winter (JJA) computed for each Brazilian Navy warning subarea along the study domain's coast (Fig. 1) based on the CMEMS wave products (product ref. nos. 1 and 2; Table 1). The trends are presented in the legend, and the units are number per year, $10^{-1} \text{ s yr}^{-1}$, and $10^{-1} \text{ kW m}^{-1} \text{ yr}^{-1}$, respectively. The abbreviations “n.s.” and “sig.” in the legend mean “not significant” and “significant”, respectively, according to the Mann–Kendall test (p value ≤ 0.05).

Moreover, coastal hazards can also occur after a sequence of events that result in a more vulnerable coast due to the lack of recovery time (Souza et al., 2019). For instance, these additional elements to coastal erosion can explain why the total increase in wave-forced events recorded on the coast in 29 years (145 %) is much larger than the increase in subarea C ($\sim 20\%$). In this case, the human-made modification of the shoreline may intensify the damaging effects of the increase in extreme wave events (Muehe, 2018).

4 Conclusion

The present work aims to assess changes in the extreme wave climate in the SWSA, giving new insights into offshore coastal risk assessment and management in this domain. Understanding the extreme wave changes is crucial for supporting future projections, which are indispensable for the design and safety control of ship vessels, offshore and coastal structures and maintenance (e.g. oil/gas platforms, aquaculture, wind and wave farms), and coastal infrastructure (e.g. ports, roads, and touristic facilities) (e.g. Bitner-Gregersen

et al., 2018; Vettor and Guedes Soares, 2020). Our findings show important changes in the SWSA mainly associated with an increase in the mean H_s values and wave period. These changes directly impact the offshore and coastal zone, increasing the wave power reaching the region and, consequently, aggravating the coastal hazards along the coast.

Even though extreme waves have a major role in coastal flooding and coastal erosion (e.g. Parise et al., 2009; Machado and Calliari, 2016), there still exists a lack of knowledge about how observed large- to regional-scale trends will affect the coast. Most of the Brazilian Navy's monitoring and warning subareas within MetArea V (WMO) require attention regarding wave climate changes. According to the WAVERYS hindcast analysis, the number of extreme wave events (above the 95th percentile $H_{s_{\text{peaks}}}$) increased in subareas A, C, and D, and the mean wave power increased in subareas B, C, and D. The trends vary depending on whether the whole period or only wintertime is considered. In this work, we analyse the winter (JJA) since it shows the most extreme wave patterns, but an extension of the analysis to other seasons is recommended for the future as the autumn

Table 2. The number of coastal hazards reported by the BDe-BS (product ref. no. 3; Table 1) in the whole period (1993–2021) and in the winter (JJA). The percentage calculation is based on the total number of events, which represents the sum of events forced only by waves, only by anomalous tides (by either astronomical or meteorological components), or by a combination of both (“waves + tides”). The last row highlights all events associated with waves, with or without tidal influence (“waves”). The trend unit is events per year or season, and bold values denote significance (Mann–Kendall test, p value ≤ 0.05).

	Whole period		Winter (JJA)	
	Number of events	Trend (number per year)	Number of events	Trend (number per season)
Total	163 (100 %)	0.23	55 (100 %)	0.14
Wave + tides	49 (30 %)	0.10	19 (35 %)	0.06
Only waves	78 (48 %)	0.12	32 (58 %)	0.06
Only tides	36 (22 %)	0.01	4 (7 %)	0.01
Waves	127 (78 %)	0.22	51 (93 %)	0.12

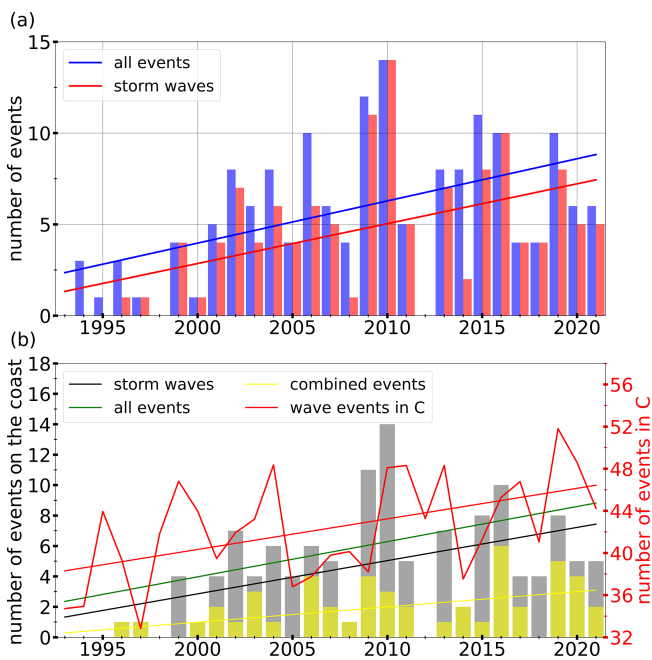


Figure 5. (a) Number of coastal hazards per year caused by any forcing (blue) and waves (red) based on BDe-BS (product ref. no. 3; Table 1). (b) Numbers and trends of coastal hazards per year associated with waves (grey bars and black line) and combined events (waves + tides; yellow bars and lines) based on BDe-BS and total number and trend of wave events in subarea C (red lines) based on the CMEMS wave products (product ref. nos. 1 and 2; Table 1). The trends presented in these panels are statistically significant (Mann–Kendall test, p value ≤ 0.05), and the values are shown in Table 2.

(MAM) and spring (SON) weather patterns are also able to produce severe waves (e.g. Crespo et al., 2022). By our findings, we recommend special attention to subareas C and D as they present changes in both the number of events and wave power.

Regarding the coastal assessment, we found an increase in the number of coastal hazards in the State of São Paulo. According to our analysis, the increase in coastal hazards in

this location is mainly associated with wave forcing and can be related to the increase in the number of extreme wave events in subarea C. Despite the well-known limitation in wave modelling, particularly to extreme waves (e.g. Campos et al., 2018), this finding provides evidence that the WEVERYS hindcast may be useful to assess not only extreme wave climate in the study domain (as shown by Crespo et al., 2022) but also the events reaching the coast in the long to medium term. However, more care is needed for interannual and interseasonal analyses that require year-by-year assessment, especially because a coastal hazard depends not only on the waves. Sea level rise, both in climatic and synoptic scales, and astronomical tides play a large role, potentially turning moderate waves into damaging ones as a high sea level allows waves to propagate and break further into the continent. Souza et al. (2019) highlighted that the most severe coastal hazards reported in the region do not present the highest values of H_s or sea level elevation but a combination of factors. Many other elements, such as coastal vulnerability, precipitation, morphology, and coastline orientation, affect the establishment of a coastal hazard (e.g. Muehe, 2018; Souza et al., 2019), mainly when the hazard is defined by its impact on the coast and not by some pure meteorological and/or oceanographic parameter.

Therefore, a complete assessment of coastal impacts needs more specific analysis considering local information and data, which is impracticable in this work, considering the study domain size. However, the trends derived herein are a valuable factor in identifying areas potentially vulnerable to climate change hazards and are also useful for engineers and stakeholders working towards the sustainable development of maritime activities. These changes may require adaptation measures, such as enhancing coastal protection (e.g. building dikes and establishing harbour protection measures). The findings reported in this work may also support the design of new projects and future assessments that will allow the advancement of the association of large-scale wave climate with coastal impacts.

Code and data availability. The data products used in this article, as well as their names and documentation, are summarised in Table 1. The wave products are available through the Copernicus Marine Service (<https://doi.org/10.48670/moi-00022>, EU Copernicus Marine Service Product, 2021; <https://doi.org/10.48670/moi-00017>, EU Copernicus Marine Service Product, 2022). The Baixada Santista Coastal Hazards database (BDe-BS) is available upon request by email to Celia R. G. Souza (celia@sp.gov.br). Codes are available upon request by email to the corresponding author.

Author contributions. CBG: conceptualisation, formal analysis, methodology, visualisation, writing – original draft. JS: conceptualisation, methodology, writing – review and editing, supervision. CRGS and PLS: methodology, writing – review. RC and PLdSD: writing – editing, supervision.

Competing interests. The contact author has declared that none of the authors has any competing interests.

Disclaimer. Publisher’s note: Copernicus Publications remains neutral with regard to jurisdictional claims in published maps and institutional affiliations.

Acknowledgements. The authors would like to acknowledge Marcel Ricker for his support with the wave event method implementation. The study was supported by the European Green Deal project “Large scale RESToration of COASTal ecosystems through rivers to sea connectivity” (REST-COAST) (grant no. 101037097). We gratefully acknowledge the project DOORS (grant no. 101000518) and DAM Mission project CostalFuture. Carolina B. Gramscianinov is funded by the Helmholtz European Partnering “Research Capacity Building for healthy, productive and resilient Seas” (SEAReCap) (grant no. PIE-0025). This study also used data and resources from the projects “Resposta Morfodinâmica de Praias do Sudeste Brasileiro aos Efeitos da Elevação do Nível do Mar e Eventos Meteorológico-Oceanográficos Extremos até 2100” (Coordenação de Aperfeiçoamento de Pessoal de Nível Superior – Brazil (CAPES) – finance code 88887.139056/2017-00), “Sistema de Aviso de Ressacas e Inundações Costeiras para o Litoral de São Paulo, com foco em Impactos das Mudanças Climáticas” (São Paulo Research Foundation, FAPESP; grant no. 2018/14601-0), and “Extreme wind and wave modelling and statistics in the Atlantic Ocean” (FAPESP; grant nos. 2018/08057-5 and 2020/01416-0).

Financial support. This research has been supported by the Helmholtz European Partnering programme (grant no. PIE-0025), H2020 Societal Challenges programme (grant nos. 101037097 and 101000518), and the Fundação de Amparo à Pesquisa do Estado de São Paulo (grant nos. 2018/14601-0, 2018/08057-5, and 2020/01416-0).

Review statement. This paper was edited by Marta Marcos and reviewed by Alejandro Orfila and one anonymous referee.

References

- ANTAQ: Anuário da Agência Nacional de Transportes Aquaviários (ANTAQ), Annual Report of the National Water Transportation Agency, Brazil, <https://anuario.antaq.gov.br>, last access: 12 May 2022 (in Portuguese).
- Aouf, L.: EU Copernicus Marine Service Quality Information Document for Global Ocean Waves Analysis and Forecasting Product, GLOBAL_ANALYSISFORECAST_WAV_001_027, Issue 3, Mercator Ocean International, <https://catalogue.marine.copernicus.eu/documents/QUID/CMEMS-GLO-QUID-001-027.pdf> (last access: 5 April 2023), 2022.
- Ardhuin, F., Rogers, E., Babanin, A. V., Filipot, J.-F., Magne, R., Roland, A., van der Westhuysen, A., Queffelec, P., Lefevre, J.-M., Aouf, L., and Collard, F.: Semiempirical Dissipation Source Functions for Ocean Waves. Part I: Definition, Calibration, and Validation, *J. Phys. Oceanogr.*, 40, 1917–1941, <https://doi.org/10.1175/2010jpo4324.1>, 2010.
- Belmonte Rivas, M. and Stoffelen, A.: Characterizing ERA-Interim and ERA5 surface wind biases using ASCAT, *Ocean Sci.*, 15, 831–852, <https://doi.org/10.5194/os-15-831-2019>, 2019.
- Bitner-Gregersen, E. M., Vanem, E., Gramstad, O., Hørte, T., Aarnes, O. J., Reistad, M., Breivik, Ø., Magnusson, A. K., and Natvig, B.: Climate change and safe design of ship structures, *Ocean Eng.*, 149, 226–237, <https://doi.org/10.1016/j.oceaneng.2017.12.023>, 2018.
- Caires, S. and Sterl, A.: 100-year return value estimates for ocean wind speed and significant wave height from the ERA-40 data, *J. Climate*, 18, 1032–1048, <https://doi.org/10.1175/JCLI-3312.1>, 2005.
- Campos, R. M., Alves, J. H. G. M., Guedes Soares, C., Guimaraes, L. G., and Parente, C. E.: Extreme wind-wave modeling and analysis in the South Atlantic ocean, *Ocean Model.*, 124, 75–93, <https://doi.org/10.1016/j.ocemod.2018.02.002>, 2018.
- Chawla, A., Spindler, D. M., and Tolman, H. L.: Validation of a thirty year wave hindcast using the Climate Forecast System Reanalysis winds, *Ocean Model.*, 70, 189–206, <https://doi.org/10.1016/j.ocemod.2012.07.005>, 2013.
- Crespo, N. M., da Silva, N. P., Palmeira, R. M. d. J., Cardoso, A. A., Kaufmann, C. L. G., Lima, J. A. M., Androni, M., de Camargo, R., and da Rocha, R. P.: Western South Atlantic Climate Experiment (WeSACEx): extreme winds and waves over the Southeastern Brazilian sedimentary basins, *Clim. Dynam.*, 60, 571–588, <https://doi.org/10.1007/s00382-022-06340-y>, 2022.
- Dalagnol, R., Gramscianinov, C. B., Crespo, N. M., Luiz, R., Chiquetto, J. B., Marques, M. T. A., Neto, G. D., de Abreu, R. C., Li, S., Lott, F. C., Anderson, L. O., and Sparrow, S.: Extreme rainfall and its impacts in the Brazilian Minas Gerais state in January 2020: Can we blame climate change?, *Climate Resilience and Sustainability*, 1, 1–15, <https://doi.org/10.1002/cli2.15>, 2022.
- Dalphinnet, A., Aouf, L., Law-Chune, S., Tressol, M., and Fernandez, E.: EU Copernicus Marine Service Product User Manual for Global Ocean Waves Analysis and Forecasting Product, GLOBAL_ANALYSISFORECAST_WAV_001_027, Issue

- 1.3, Mercator Ocean International, <https://catalogue.marine.copernicus.eu/documents/PUM/CMEMS-GLO-PUM-001-027.pdf> (last access: 5 April 2023), 2022.
- da Rocha, R. P., Sugahara, S., and da Silveira, R. B.: Sea Waves Generated by Extratropical Cyclones in the South Atlantic Ocean: Hindcast and Validation against Altimeter Data, *Weather Forecast.*, 19, 398–410, [https://doi.org/10.1175/1520-0434\(2004\)019<0398:swgbec>2.0.co;2](https://doi.org/10.1175/1520-0434(2004)019<0398:swgbec>2.0.co;2), 2004.
- De Leo, F., Solari, S., and Besio, G.: Extreme wave analysis based on atmospheric pattern classification: an application along the Italian coast, *Nat. Hazards Earth Syst. Sci.*, 20, 1233–1246, <https://doi.org/10.5194/nhess-20-1233-2020>, 2020.
- Dobrynin, M., Murawsky, J., and Yang, S.: Evolution of the global wind wave climate in CMIP5 experiments, *Geophys. Res. Lett.*, 39, L18606, <https://doi.org/10.1029/2012GL052843>, 2012.
- Dragani, W. C., Cerne, B. S., Campetella, C. M., Possia, N. E., and Campos, M. I.: Synoptic patterns associated with the highest wind-waves at the mouth of the Río de la Plata estuary, *Dynam. Atmos. Oceans*, 61–62, 1–13, <https://doi.org/10.1016/j.dynatmoce.2013.02.001>, 2013.
- EU Copernicus Marine Service Product: Global Ocean Waves Reanalysis (WAVERYS), Mercator Ocean International [data set], <https://doi.org/10.48670/moi-00022>, 2021.
- EU Copernicus Marine Service Product: Global Ocean Waves Analysis and Forecasting Product, Mercator Ocean International [data set], <https://doi.org/10.48670/moi-00017>, 2022.
- Godoi, V. A. and Torres Júnior, A. R.: A global analysis of austral summer ocean wave variability during SAM–ENSO phase combinations, *Clim. Dynam.*, 54, 3991–4004, <https://doi.org/10.1007/s00382-020-05217-2>, 2020.
- Godoi, V. A., de Andrade, F. M., Durrant, T. H., and Torres Júnior, A. R.: What happens to the ocean surface gravity waves when ENSO and MJO phases combine during the extended boreal winter?, *Clim. Dynam.*, 54, 1407–1424, <https://doi.org/10.1007/s00382-019-05065-9>, 2020.
- Gramscianinov, C. B., Hodges, K. I., and Camargo, R.: The properties and genesis environments of South Atlantic cyclones, *Clim. Dynam.*, 53, 4115–4140, <https://doi.org/10.1007/s00382-019-04778-1>, 2019.
- Gramscianinov, C. B., Campos, R. M., de Camargo, R., Hodges, K. I., Guedes Soares, C., and da Silva Dias, P. L.: Analysis of Atlantic extratropical storm tracks characteristics in 41 years of ERA5 and CFSR/CFSv2 databases, *Ocean Eng.*, 216, 108111, <https://doi.org/10.1016/j.oceaneng.2020.108111>, 2020a.
- Gramscianinov, C. B., Campos, R. M., Guedes Soares, C., and de Camargo, R.: Extreme waves generated by cyclonic winds in the western portion of the South Atlantic Ocean, *Ocean Eng.*, 213, 107745, <https://doi.org/10.1016/j.oceaneng.2020.107745>, 2020b.
- Gramscianinov, C. B., Campos, R. M., de Camargo, R., and Guedes Soares, C.: Relation between cyclone evolution and fetch associated with extreme wave events in the South Atlantic Ocean, *J. Offshore Mech. Arct.*, 143, 061202, <https://doi.org/10.1115/1.4051038>, 2021.
- Gramscianinov, C. B., de Camargo, R., Campos, R. M., Soares, C. G., and da Silva Dias, P. L.: Impact of extratropical cyclone intensity and speed on the extreme wave trends in the Atlantic Ocean, *Clim. Dynam.*, 60, 1447–1466, <https://doi.org/10.1007/s00382-022-06390-2>, 2023.
- Guillou, N.: Estimating wave energy flux from significant wave height and peak period, *Renew. Energ.*, 155, 1383–1393, <https://doi.org/10.1016/j.renene.2020.03.124>, 2020.
- Hemer, M. A., Church, J. A., and Hunter, J. R.: Variability and trends in the directional wave climate of the Southern Hemisphere, *Int. J. Climatol.*, 30, 475–491, <https://doi.org/10.1002/joc.1900>, 2010.
- Hersbach, H., Bell, B., Berrisford, P., Hirahara, S., Horányi, A., Muñoz-Sabater, J., Nicolas, J., Peubey, C., Radu, R., Schepers, D., Simmons, A., Soci, C., Abdalla, S., Abellan, X., Balsamo, G., Bechtold, P., Biavati, G., Bidlot, J., Bonavita, M., Chiara, G., Dahlgren, P., Dee, D., Diamantakis, M., Dragani, R., Flemming, J., Forbes, R., Fuentes, M., Geer, A., Haimberger, L., Healy, S., Hogan, R. J., Hólm, E., Janisková, M., Keeley, S., Laloyaux, P., Lopez, P., Lupu, C., Radnoti, G., Rosnay, P., Rozum, I., Vamborg, F., Villaume, S., and Thépaut, J.-N.: The ERA5 global reanalysis, *Q. J. Roy. Meteor. Soc.*, 146, 1999–2049, <https://doi.org/10.1002/qj.3803>, 2020.
- Hoskins, B. J. and Hodges, K. I.: A New Perspective on Southern Hemisphere Storm Tracks, *J. Climate*, 18, 4108–4129, <https://doi.org/10.1175/JCLI3570.1>, 2005.
- ICMBio: Atlas dos Manguezais do Brasil (Brazilian Mangrove Atlas), Instituto Chico Mendes de Conservação da Biodiversidade (ICMBio), Ministério do Meio Ambiente – MMA (Ministry of the Environment), Brazil, <https://acervo.socioambiental.org/sites/default/files/documents/17L00001.pdf> (last access: 24 April 2023), 2018 (in Portuguese).
- Kendall, M.: Rank Correlation Methods, 4th edn., Charles Griffin, London, ISBN-13: 978-01-9520-837-5, 1975.
- Law-Chune, S.: EU Copernicus Marine Service Product User Manual for the Global Ocean Wave Multi Year product, GLOBAL_REANALYSIS_WAV_001_032, Issue 1.2, Mercator Ocean International, <https://catalogue.marine.copernicus.eu/documents/PUM/CMEMS-GLO-PUM-001-032.pdf> (last access: 5 April 2023), 2022.
- Law-Chune, S., Aouf, L., Dalphiné, A., Levier, B., Drillet, Y., and Drevillon, M.: WAVERYS: a CMEMS global wave reanalysis during the altimetry period, *Ocean Dynam.*, 71, 357–378, <https://doi.org/10.1007/s10236-020-01433-w>, 2021a.
- Law-Chune, S., Aouf, L., Levier, B., and Dalphiné, A.: EU Copernicus Marine Service Quality Information Document for the Global Ocean Waves Reanalysis, GLOBAL_REANALYSIS_WAV_001_032, Issue 1.3, Mercator Ocean International, <https://catalogue.marine.copernicus.eu/documents/QUID/CMEMS-GLO-QUID-001-032.pdf> (last access: 5 April 2023), 2021b.
- Lemos, G., Semedo, A., Dobrynin, M., Behrens, A., Staneva, J., Bidlot, J.-R., and Miranda, P. M.: Mid-twenty-first century global wave climate projections: Results from a dynamic CMIP5 based ensemble, *Global Planet. Change*, 172, 69–87, <https://doi.org/10.1016/j.gloplacha.2018.09.011>, 2019.
- Linhares, P. S., Fukai, D. T., and Souza, C. R. G.: Clima de ondas e maré em três eventos meteo-oceanográficos extremos ocorridos em São Paulo, em fevereiro e abril de 2020, in: X Congresso sobre Planejamento e Gestão das Zonas Costeiras nos Países de Expressão Portuguesa, APRH/ABRhidro, 6–10 December 2021, on-line, 2021 (in Portuguese).
- Lobeto, H., Menendez, M., and Losada, I. J.: Projections of Directional Spectra Help to Unravel the Future Behavior

- of Wind Waves, *Frontiers in Marine Science*, 8, 655490, <https://doi.org/10.3389/fmars.2021.655490>, 2021.
- Machado, A. A. and Calliari, L. J.: Synoptic systems generators of extreme wind in Southern Brazil: atmospheric conditions and consequences in the coastal zone, *J. Coastal Res.*, 1, 1182–1186, <https://doi.org/10.2112/SI75-237.1>, 2016.
- Machado, A. A., Calliari, L. J., Melo, E., and Klein, A. H. F.: Historical assessment of extreme coastal sea state conditions in southern Brazil and their relation to erosion episodes, *Pan-American Journal of Aquatic Sciences*, 5, 105–114, [https://panamjas.org/pdf_artigos/PANAMJAS_5\(2\)_277-286.pdf](https://panamjas.org/pdf_artigos/PANAMJAS_5(2)_277-286.pdf) (last access: 24 April 2023), 2010.
- Mann, H. B.: Nonparametric Tests Against Trend, *Econometrica*, 13, 245–259, <http://www.jstor.org/stable/1907187> (last access: 24 April 2023), 1945.
- Marcello, F., Wainer, I., and Rodrigues, R. R.: South Atlantic Subtropical Gyre Late Twentieth Century Changes, *J. Geophys. Res.-Oceans*, 123, 5194–5209, <https://doi.org/10.1029/2018jc013815>, 2018.
- Meucci, A., Young, I. R., Hemer, M., Kirezci, E., and Ranasinghe, R.: Projected 21st century changes in extreme wind-wave events, *Science Advances*, 6, eaaz7295, <https://doi.org/10.1126/sciadv.aaz7295>, 2020.
- Muehe, D.: Panorama da Erosão Costeira no Brasil (Overview of Coastal Erosion in Brazil), Ministério do Meio Ambiente – MMA (Ministry of the Environment), Brazil, ISBN: 978-85-7738-394-8 (on line), 2018 (in Portuguese).
- Odériz, I., Silva, R., Mortlock, T. R., Mori, N., Shimura, T., Webb, A., Padilla-Hernández, R., and Villers, S.: Natural Variability and Warming Signals in Global Ocean Wave Climates, *Geophys. Res. Lett.*, 48, e2021GL093622, <https://doi.org/10.1029/2021GL093622>, 2021.
- Parise, C. K., Calliari, L. J., and Krusche, N.: Extreme storm surges in the south of Brazil: atmospheric conditions and shore erosion, *Braz. J. Oceanogr.*, 57, 175–188, 2009.
- Pereira-Filho, G. H., Mendes, V. R., Perry, C. T., Shintate, G. I., Niz, W. C., Sawakuchi, A. O., Bastos, A. C., Giannini, P. C. F., Motta, F. S., Millo, C., Paula-Santos, G. M., and Moura, R. L.: Growing at the limit: Reef growth sensitivity to climate and oceanographic changes in the South Western Atlantic, *Global Planet. Change*, 201, 103479, <https://doi.org/10.1016/j.gloplacha.2021.103479>, 2021.
- Pianca, C., Mazzini, P. L. F., and Siegle, E.: Brazilian offshore wave climate based on NWW3 reanalysis, *Braz. J. Oceanogr.*, 58, 53–70, 2010.
- Sasaki, D. K., Gramscianinov, C. B., Castro, B., and Dottori, M.: Intraseasonal variability of ocean surface wind waves in the western South Atlantic: the role of cyclones and the Pacific South American pattern, *Weather Clim. Dynam.*, 2, 1149–1166, <https://doi.org/10.5194/wcd-2-1149-2021>, 2021.
- Sen, P. K.: Estimates of the Regression Coefficient Based on Kendall's Tau, *J. Am. Stat. Assoc.*, 63, 1379–1389, <https://doi.org/10.1080/01621459.1968.10480934>, 1968.
- Silva, A. P., Klein, A. H., Fetter-Filho, A. F., Hein, C. J., Méndez, F. J., Broggio, M. F., and Dalinghaus, C.: Climate-induced variability in South Atlantic wave direction over the past three millennia, *Sci. Rep.-UK*, 10, 1–12, <https://doi.org/10.1038/s41598-020-75265-5>, 2020.
- Souza, C. R. d. G., Souza, A. P., and Harari, J.: Long Term Analysis of Meteorological-Oceanographic Extreme Events for the Baixada Santista Region, in: *Climate Change in Santos Brazil: Projections, Impacts and Adaptation Options*, Springer International Publishing, 97–134, https://doi.org/10.1007/978-3-319-96535-2_6, 2019.
- Souza, C. R. G., Linhares, P. S., and Morais Silva, V. A.: Histórico de Eventos Meteorológicos-Oceanográficos Intensos/Extremos na Costa de São Paulo (Brasil): 1928–2021, in: *Libro Resúmenes. Congreso Latinoamericano de Ciencias del Mar, XIX COLACMAR, Asociación Latinoamericana de Investigadores en Ciencias del Mar*, 19 al 23 de septiembre 2022, Ciudad de Panamá, Panamá, 2022 (in Portuguese).
- Staneva, J., Ricker, M., Akpınar, A., Behrens, A., Giesen, R., and von Schuckmann, K.: Long-term interannual changes in extreme winds and waves in the Black Sea, *J. Oper. Oceanogr.*, 15, 56–64, <https://doi.org/10.1080/1755876X.2022.2095169>, 2022.
- Vettor, R. and Guedes Soares, C.: A global view on bimodal wave spectra and crossing seas from ERA-Interim, *Ocean Eng.*, 210, 107439, <https://doi.org/10.1016/j.oceaneng.2020.107439>, 2020.
- Wang, F., Shao, W., Yu, H., Kan, G., He, X., Zhang, D., Ren, M., and Wang, G.: Re-evaluation of the Power of the Mann-Kendall Test for Detecting Monotonic Trends in Hydrometeorological Time Series, *Frontiers in Earth Science*, 8, 14, <https://doi.org/10.3389/feart.2020.00014>, 2020.
- Weisse, R. and Günther, H.: Wave climate and long-term changes for the Southern North Sea obtained from a high-resolution hindcast 1958–2002, *Ocean Dynam.*, 57, 161–172, <https://doi.org/10.1007/s10236-006-0094-x>, 2007.
- Young, I. R. and Ribal, A.: Multiplatform evaluation of global trends in wind speed and wave height, *Science*, 364, 548–552, <https://doi.org/10.1126/science.aav9527>, 2019.
- Zamboni, A. and Nicolodi, J. L.: Macrodiagnóstico da Zona Costeira e Marinha do Brasil (Macrodiagnosis of the Brazilian Coastal and Marine Zone), Ministério do Meio Ambiente – MMA (Ministry of the Environment), Brazil, ISBN: 978-85-7738-112-8, 2008 (in Portuguese).